

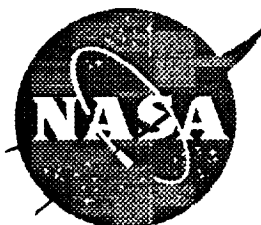
NASA Technical Memorandum 109015

11-39
193183
30P

**DEVELOPMENT AND COMPARISON OF ADVANCED
REDUCED-BASIS METHODS FOR THE TRANSIENT STRUCTURAL
ANALYSIS OF UNCONSTRAINED STRUCTURES**

**DAVID M. McGOWAN
SUSAN W. BOSTIC
CHARLES J. CAMARDA**

NOVEMBER 1993



(NASA-TM-109015) DEVELOPMENT AND
COMPARISON OF ADVANCED
REDUCED-BASIS METHODS FOR THE
TRANSIENT STRUCTURAL ANALYSIS OF
UNCONSTRAINED STRUCTURES (NASA)
30 p

N94-17259

Unclas

G3/39 0193183

National Aeronautics and
Space Administration

Langley Research Center
Hampton, Virginia 23681-0001



Abstract

The development of two advanced reduced-basis methods, the force-derivative method and the Lanczos method, and modifications to two widely used modal methods, the mode-displacement method and the mode-acceleration method for transient structural analysis of unconstrained structures are presented. Two example structural problems are studied: an undamped, unconstrained beam subject to a uniformly distributed load which varies as a sinusoidal function of time and an undamped high-speed civil transport aircraft subject to a normal wing tip load which varies as a sinusoidal function of time. These example problems are used to verify the methods and to compare the relative effectiveness of each of the four reduced-basis methods for performing transient structural analyses on unconstrained structures. The methods are verified with a solution obtained by directly integrating the full system of equations of motion, and they are compared using the number of basis vectors required to obtain a desired level of accuracy and the associated computational times as comparison criteria.

Introduction

The transient analysis of complex structures that are modeled as discrete, multidegree-of-freedom systems often requires the solution of very large, coupled systems of equations. Calculation of the transient structural response for such large systems is computationally expensive and, as a result, methods that can significantly reduce the problem size and computational cost and still retain solution accuracy are highly desirable. A class of methods, called reduced-basis methods, has been developed which approximates the solution of the complete system of equations using a much smaller or reduced set of generalized basis vectors¹⁻⁵. Examples of basis vectors that have been investigated include: eigenvectors¹⁻⁴, Ritz vectors⁵, Lanczos vectors⁶, and combinations of the above⁷. A reduced-basis method that uses the eigenvectors of a system is referred to herein as a modal method. Similarly, a reduced-basis method that uses Lanczos vectors as basis vectors is referred to herein as the Lanczos method.

Recently, a comparison was made of four reduced-basis methods for transient structural analysis.⁸ The methods studied included two widely used modal methods, the mode-displacement method (MDM) and the mode-acceleration method (MAM). Two advanced reduced-basis methods, including a higher-order modal method referred to as the force-derivative method (FDM) and the Lanczos method, were also studied. The relative merits of each of these methods are discussed in reference 8. These four methods were compared in terms of the number of basis vectors required to obtain a desired level of accuracy and the associated computational times. The results indicate that, in general, the FDM is the most effective method in terms of the number of basis vectors required for an accurate solution and the associated computational time.

The purpose of the present study is to extend the work of reference 8 to include the analysis of unconstrained (free-free) structures. The analysis of

such structures using the previously mentioned reduced-basis methods must account for the rigid-body motion of the structure. Analyses using the MAM, the FDM and the Lanczos method are further complicated by the fact that the stiffness matrix of the system is singular and cannot be inverted. Since these three methods use the inverse of the stiffness matrix, the development of the theory for these methods must be modified. The present paper describes the necessary modifications to the theory for all the reduced-basis methods considered and presents applications of these methods to two example problems. The scope of the example problems presented in the present report is not intended to be exhaustive since several of the problem parameters considered in reference 8 are not considered here. These parameters include: the time variation of the forcing function, the inclusion of different types of damping (i.e., proportional and non-proportional), and the spatial distribution of the forcing function. The two problems were selected to verify the modified theories and to enable a limited comparison of the methods to be made.

As in reference 8, the four reduced-basis methods are compared in terms of the number of basis vectors required to achieve a desired level of accuracy, as well as the associated computational time for each method. The approximate solutions obtained using the modified reduced-basis methods are verified with and compared to a full-system solution calculated by directly integrating the full system of equations of motion using the Newmark-Beta implicit time integration method. The four reduced-basis methods have been implemented on a CONVEX C220 high-performance computer using the COmputational MEchanics Testbed (COMET)⁹ as a general-purpose finite-element code.

Symbols

| | |
|-------|--|
| a | flexibility matrix, $a = K^{-1}$ |
| a_E | elastic flexibility matrix |
| C | damping matrix |
| e | spatial error norm |
| E | modulus of elasticity |
| f | force vector |
| I | identity matrix, moment of inertia |
| K | stiffness matrix |
| L | length |
| M | mass matrix, moment |
| m | subset of total number of degrees-of-freedom, $m \ll n$ |
| n | total number of degrees-of-freedom |
| N_E | number of elastic degrees-of-freedom |
| N_R | number of rigid-body degrees-of-freedom |
| q_i | i th Lanczos vector |
| Q | matrix of Lanczos vectors |
| T_m | tridiagonal matrix generated by Lanczos-vector-based eigensolver |
| t | time |
| u | displacement |
| x_i | i th generalized coordinate |

x vector of generalized coordinates
 y_i i th basis vector
 Y matrix of basis vectors

Greek

α, β Integration constants for Newmark-Beta method
 Δt time step used in Newmark-Beta time integration
 ζ_i i th modal viscous damping factor
 Λ matrix of damping coefficients ($\Lambda = \Phi^T C \Phi$), see Eq. (5b)
 ρ density
 ϕ_i i th undamped eigenvector
 Φ matrix of undamped eigenvectors
 ω_i i th undamped natural frequency
 Ω diagonal matrix of undamped natural frequencies

Subscripts

a approximate solution, see Eq. (38)
 E elastic
 f full-system solution, see Eq. (38)
 R rigid-body
 S stress

Superscripts

\cdot derivative with respect to time
 \wedge reduced set of m basis vectors, eigenvalues, or generalized coordinates
 T transpose

Determination of the Full-System Solution

The approximate solutions obtained using the four modified reduced-basis methods are verified with and compared to a full-system solution obtained by integrating directly the full system of equations of motion using the Newmark-Beta implicit time-integration method. The equations of motion to be solved represent a damped, linear, structural system with n degrees-of-freedom, and they can be written in discrete form as

$$M\ddot{u} + C\dot{u} + Ku = f(t) \tag{1}$$

where

M, C and K are $(n \times n)$ matrices
 \ddot{u} is the acceleration vector $(n \times 1)$
 \dot{u} is the velocity vector $(n \times 1)$
 u is the displacement vector $(n \times 1)$

and

$f(t)$ is the load vector ($n \times 1$)

Although the theory presented herein includes damping, only undamped structures are considered in the present study. The damping matrix, C , used in the present study will take one of two forms depending upon whether or not the damping is proportional or non-proportional. If the damping is proportional, with a modal viscous damping factor ζ_i defined for each of the first m modes of the system, the damping matrix is calculated to be (see reference 10)

$$C = \sum_{i=1}^m 2\zeta_i \omega_i (M\phi_i)(M\phi_i)^T \quad (2)$$

If the damping is non-proportional (i.e., containing discrete dampers), the damping matrix will be diagonal with the damping factors of the dashpots inserted into the correct positions of the matrix. For example, a translational damper with a damping factor of 0.8 in-sec at node 1 of a beam with two degrees-of-freedom at each node would result in a value of 0.8 being placed in the $C(1,1)$ position.

The system of equations given in Eq. (1) is solved at discrete times using the Newmark-Beta method as described in references 10 and 11 to yield the full-system solution. The method is used with assumed values of the integration constants α and β to be 0.25 and 0.50, respectively. Therefore, the method is equivalent to the trapezoidal rule or the constant-average-acceleration method¹⁰⁻¹¹. The time step, Δt , is equal to 0.0001 sec. This value was selected by conducting several analyses of a cantilevered beam example problem while successively decreasing the time step until no appreciable change in the full-system solution was apparent. For large problems, the direct integration of the full system of equations can be prohibitively expensive in terms of computational cost.

Reduced-Basis Methods for Constrained Structures

A review of the general theory of reduced-basis methods is given in reference 8. The equations for the four methods considered in the present study as well as descriptions of each method are also given in reference 8. For completeness, these equations are repeated here and a brief description of each method is given.

Modal methods

The three modal methods studied in the present paper are the mode-displacement method (MDM), the mode-acceleration method (MAM), and the force-derivative method (FDM). A unified derivation of all of these methods is presented in references 12-14. This derivation clarifies the mathematical relationship between the three methods and shows that the MDM may be considered to be a zeroth-order form of the FDM, and the MAM may be

considered to be a first-order form of the FDM. For the MDM, the displacement, $u(t)$, is approximated by the superposition of a subset of m eigenvectors of the system scaled by a set of generalized coordinates known as modal coordinates, as shown in Eq. (3).

$$u(t) \approx \sum_{i=1}^m \phi_i x_i(t) \approx \hat{\Phi} \hat{x}(t) \quad (m \ll n) \quad (\text{order } 0) \quad (3)$$

where

ϕ_i is the i th undamped natural eigenvector ($n \times 1$)
 $x_i(t)$ is the i th modal coordinate (scalar)
 $\hat{\Phi}$ is an ($n \times m$) matrix whose columns contain the undamped natural eigenvectors

and

$\hat{x}(t)$ is an ($m \times 1$) vector containing the modal coordinates.

For structural systems where M , C and K are symmetric, the modal coordinates, $\hat{x}(t)$, are obtained by solving

$$\bar{M} \hat{\ddot{x}}(t) + \bar{C} \hat{\dot{x}}(t) + \bar{K} \hat{x}(t) = \bar{f}(t) \quad (m \times m) \quad (4)$$

where

$$\bar{M} = \hat{\Phi}^T M \hat{\Phi} = I \quad (5a)$$

$$\bar{C} = \hat{\Phi}^T C \hat{\Phi} = \hat{\Lambda} \quad (5b)$$

$$\bar{K} = \hat{\Phi}^T K \hat{\Phi} = \hat{\Omega}^2 \quad (5c)$$

and

$$\bar{f}(t) = \hat{\Phi}^T f(t) \quad (5d)$$

The displacement response may then be obtained by substituting the modal coordinates, $\hat{x}(t)$, into Eq. (3).

The MAM was developed to improve the convergence of the stress solutions from the MDM. The MAM is a first-order method that contains the results from the zeroth-order MDM plus an additional term, and, as shown in references 12-14, can be put into the following form

$$u(t) \approx \hat{\Phi} \hat{x} + (K^{-1} - \hat{\Phi} \hat{\Omega}^{-2} \hat{\Phi}^T) f(t) \quad (\text{order } 1) \quad (6)$$

The last term in Eq. (6) is called a pseudo-static correction term because it contains the static displacement of the system, $K^{-1}f(t)$, and an additional correction factor. This term serves to approximate the flexibility of the higher modes that are neglected by using a reduced set of modes in the analysis¹⁰.

The force-derivative method (FDM) is a higher-order modal method that was developed to improve the convergence rates of the MDM and the MAM. A second-order expression of the FDM is given by

$$u(t) \approx \hat{\Phi}\hat{x} + (K^{-1} - \hat{\Phi}\hat{\Omega}^{-2}\hat{\Phi}^T)f(t) - (K^{-1}CK^{-1} - \hat{\Phi}\hat{\Omega}^{-2}\hat{\Lambda}\hat{\Omega}^{-2}\hat{\Phi}^T)\dot{f}(t) \quad (\text{order } 2) \quad (7)$$

As shown in Eq. (7), the second-order form consists of the first-order MAM plus a higher-order term multiplied by the first derivative of the forcing function with respect to time. As for the case of the MAM, the additional term serves to approximate better the flexibility of the higher modes that are neglected by the use of a reduced set of modes. Furthermore, increasing the order of the approximation results in the addition of higher-order terms multiplied by successively higher-order time derivatives of the forcing function¹²⁻¹⁴. Hence, the order of the FDM used is dependent upon the number of time derivatives of the forcing function that exist. For example, if the forcing function is described by a quadratic function of time, (for which there exists a maximum of two non-zero time derivatives), the highest-order FDM that will yield useful results is order 3. If an order higher than three is used, all the additional terms (past order 3) would be zero. The form of the FDM used in Eq. (7) was shown in references 12-14 to be valid for both proportional and non-proportional damping.

Lanczos method

The Lanczos method uses Lanczos vectors as basis vectors instead of using undamped natural eigenvectors as basis vectors. The Lanczos vectors are obtained using the Lanczos algorithm as described in references 6 and 15-18. Besides the Lanczos vectors, the Lanczos algorithm produces the terms of a tridiagonal matrix¹⁷⁻¹⁸, T_m , of order m . The use of the Lanczos vectors and T_m in the transient analysis is described subsequently.

For this method, the displacements, $u(t)$, are approximated by the superposition of a set of m Lanczos vectors scaled by a set of generalized coordinates known as Lanczos coordinates

$$u(t) \approx \sum_{i=1}^m q_i x_i(t) \approx \hat{Q} \hat{x}(t) \quad (m \ll n) \quad (8)$$

where

- q_i is the i th Lanczos vector ($n \times 1$)
- $x_i(t)$ is the i th Lanczos coordinate (scalar)
- \hat{Q} is an ($n \times m$) matrix whose columns contain the Lanczos vectors

and

$\hat{x}(t)$ is an ($m \times 1$) vector containing the Lanczos coordinates.

As with the modal methods, the Lanczos coordinates may be obtained by solving Eq. (4) with the barred terms as defined by Eqs. (9).

$$\bar{M} = \hat{Q}^T M K^{-1} M \hat{Q} = T_m \quad (9a)$$

$$\bar{C} = \hat{Q}^T M K^{-1} C \hat{Q} \quad (9b)$$

$$\bar{K} = \hat{Q}^T M \hat{Q} = I \quad (9c)$$

and

$$\bar{f}(t) = \hat{Q}^T M K^{-1} f(t) \quad (9d)$$

The displacement response may then be obtained by substituting the Lanczos coordinates, $\hat{x}(t)$, into Eq. (8).

Reduced-Basis Methods for Unconstrained Structures

The theory presented for the MDM, the MAM, the FDM and the Lanczos method must be modified to allow for the analysis of unconstrained (free-free) structures. One reason that the theory must be modified is that the rigid-body displacements must be calculated and included in the transient response of the structure. Another reason for modifying the theory is that the stiffness matrix for an unconstrained system is singular and cannot be inverted. Since the MAM, the FDM, and the Lanczos method use the inverse of the stiffness matrix, modifications must be made to the theory for these methods to account for this singularity. A discussion of the modified theory for each of the methods is presented subsequently.

Mode-displacement method (MDM)

The modifications to the theory for the MDM presented herein follow those given in reference 10. However, the theory presented herein includes systems with damping, while the theory presented in reference 10 does not. The displacement, $u(t)$, of an n -degree-of-freedom system with N_R rigid-body modes and N_E elastic modes (i.e., $n = N_R + N_E$) is equal to the sum of the rigid-body displacements, $u_R(t)$ and the elastic displacements, $u_E(t)$, as shown in Eq. (10).

$$u(t) = u_R(t) + u_E(t) \quad (10)$$

The rigid-body displacements can be written as the superposition of the rigid-body modes scaled by a set of rigid-body coordinates, and the elastic displacements can be written as the superposition of the elastic modes scaled by a set of elastic coordinates, as shown in Eqs. (11).

$$u_R(t) = \Phi_R x_R(t) \quad (11a)$$

and

$$u_E(t) = \Phi_E x_E(t) \quad (11b)$$

where

Φ_R is an $(n \times N_R)$ matrix whose columns contain the rigid-body modes

$x_R(t)$ is an $(N_R \times 1)$ vector containing the rigid-body coordinates

Φ_E is an $(n \times N_E)$ matrix whose columns contain the elastic modes

and

$x_E(t)$ is an $(N_E \times 1)$ vector containing the elastic coordinates.

Substituting Eqs. (11) into Eq. (10) yields

$$u(t) = u_R(t) + u_E(t) = \Phi_R x_R(t) + \Phi_E x_E(t) \quad (12)$$

Substituting Eq. (10) into the equations of motion, Eq. (1), and noting that $Ku_R = 0$ results in the following equation

$$M\ddot{u}_R + C\dot{u}_R + M\ddot{u}_E + C\dot{u}_E + Ku_E = f(t) \quad (13)$$

Substituting Eq. (11a) into Eq. (13), and premultiplying by Φ_R^T yields

$$\bar{M}_R \ddot{x}_R + \bar{C}_R \dot{x}_R = \Phi_R^T f(t) \quad (14)$$

where

$$\bar{M}_R = \Phi_R^T M \Phi_R = I \quad (15a)$$

$$\bar{C}_R = \Phi_R^T C \Phi_R \quad (15b)$$

However, noting the definition of C given in Eq. (2) and the orthogonality condition expressed in Eq. (15a), it may be shown that $\bar{C}_R = 0$ for proportional damping. Similarly, substituting Eq. (11b) into Eq. (13), and premultiplying by Φ_E^T yields

$$\bar{M}_E \ddot{x}_E + \bar{C}_E \dot{x}_E + \bar{K}_E x_E = \Phi_E^T f(t) \quad (16)$$

where

$$\bar{M}_E = \Phi_E^T M \Phi_E = I \quad (17a)$$

$$\bar{C}_E = \Phi_E^T C \Phi_E = \Lambda \quad (17b)$$

and

$$\bar{K}_E = \Phi_E^T K \Phi_E = \Omega_E^2 \quad (17c)$$

To determine the displacements using the MDM, Eq. (12) is used with all of the rigid-body modes and a reduced set of m elastic modes, where m is typically much smaller than N_E . Therefore,

$$u(t) = u_R(t) + \hat{u}_E(t) = \Phi_R x_R(t) + \hat{\Phi}_E \hat{x}_E(t) \quad (\text{order } 0) \quad (18)$$

where

$\hat{u}_E(t)$ is an $(m \times 1)$ vector containing the approximate elastic displacements

$\hat{\Phi}_E$ is an $(n \times m)$ matrix whose columns contain the m elastic modes

and

$\hat{x}_E(t)$ is an $(m \times 1)$ vector containing the m elastic coordinates.

The rigid-body coordinates, $x_R(t)$, are calculated by integrating Eq. (14) using all of the rigid-body modes, and the elastic coordinates, $\hat{x}_E(t)$, are calculated by integrating Eq. (16), using a reduced set of m elastic modes. The displacements, $u(t)$, are then calculated by substituting these coordinates into Eq. (18).

Mode-acceleration method (MAM) and force-derivative method (FDM)

Since the stiffness matrix for an unconstrained system is singular and cannot be inverted, the MAM and FDM cannot be used in the forms given in Eqs. (6) and (7) because the static-displacement term, $K^{-1}f(t)$, cannot be calculated. As a result of this singularity, the theory for the MAM and FDM must be modified. The modifications that have been made to the theory are described subsequently, and they follow those given in reference 10. However, damping is included in the theory presented herein, while it is neglected in reference 10.

Mode-acceleration method (MAM)

Solving Eq. (16) for $x_E(t)$ and substituting the resulting expression into Eq. (12) yields

$$u(t) = \Phi_R x_R(t) + (\Phi_E \bar{K}_E^{-1} \Phi_E^T) f(t) - (\Phi_E \bar{K}_E^{-1} \bar{M}_E) \ddot{x}_E(t) - (\Phi_E \bar{K}_E^{-1} \bar{C}_E) \dot{x}_E(t) \quad (19)$$

The first term in Eq. (19) is exactly equal to the rigid-body term in the mode-displacement method since all of the rigid-body modes are used. To derive an expression for the MAM, the last two terms of Eq. (19) are truncated to use a reduced set of m elastic modes. The resulting equation is

$$u(t) \approx \Phi_R x_R(t) + (\Phi_E \bar{K}_E^{-1} \Phi_E^T) f(t) - (\hat{\Phi}_E \hat{K}_E^{-1} \hat{M}_E) \hat{\ddot{x}}_E(t) - (\hat{\Phi}_E \hat{K}_E^{-1} \hat{C}_E) \hat{\dot{x}}_E(t) \quad (20)$$

Rewriting Eq. (20) in a form that is similar to that given in reference 10 yields

$$u(t) \approx \Phi_R x_R(t) + a_E f(t) - (\hat{\Phi}_E \hat{K}_E^{-1} \hat{M}_E) \hat{\ddot{x}}_E(t) - (\hat{\Phi}_E \hat{K}_E^{-1} \hat{C}_E) \hat{\dot{x}}_E(t) \quad (21)$$

where

$$a_E = \Phi_E \bar{K}_E^{-1} \Phi_E^T \quad (22)$$

The product $a_E f(t)$ in Eq. (21) is an expression for the static-displacement described previously, and is analogous to the product $K^{-1}f(t)$ in Eq. (6). An expression for the elastic flexibility matrix, a_E , is given in Eq. (22). However, computing a_E using Eq. (22) requires that all of the elastic modes be used. In reference 10, Craig derives an equivalent expression for a_E that does not require the use of all of the elastic modes. The details of this derivation are omitted here, but the equivalent expression for a_E is given in Eq. (23).

$$a_E = R^T a R \quad (23)$$

where

a_E is the elastic flexibility matrix
 a is the flexibility matrix (i.e., $a = K^{-1}$) of the system relative to some statically determinate constraints with zeros in the rows and columns corresponding to the constraints

and

$$R = I - M \Phi_R \bar{M}_R^{-1} \Phi_R^T$$

An expression for the MAM that is similar to that given in Eq. (6) may now be developed by following the alternate natural-mode formulation of the FDM given in reference 14. This formulation involves expressing the solution for the elastic modal coordinates, $\hat{x}_E(t)$, by using the Duhamel integral as shown in Eq. (24). Assuming zero initial conditions, the solution to Eq. (16) for the i th elastic modal coordinate, $x_{Ei}(t)$, may be written as

$$x_{Ei}(t) = \frac{1}{\omega_{di}} \int_0^t e^{-\zeta_i \omega_{Ei}(t-\tau)} \sin \omega_{di}(t-\tau) \Phi_{Ei}^T f(\tau) d\tau \quad (24)$$

where

$$\omega_{di} = \sqrt{\omega_{Ei}^2 - (\zeta_i \omega_{Ei})^2} \quad (25)$$

and

ζ_i is the modal viscous damping factor

A vector of m elastic coordinates, $\hat{x}_E(t)$, may be calculated using Eq. (24), and then, using Leibnitz's rule, expressions for $\dot{\hat{x}}_E(t)$ and $\ddot{\hat{x}}_E(t)$ may be obtained and substituted into Eq. (21) to yield (after simplification)

$$u(t) = \Phi_R x_R(t) + \hat{\Phi}_E \hat{x}_E(t) + (a_E - \hat{\Phi}_E \hat{\Omega}_E^{-2} \hat{\Phi}_E^T) f(t) \quad (\text{order 1}) \quad (26)$$

Therefore, the analysis of structures with rigid-body modes using the MAM requires the use of Eq. (26) with a_E defined by Eq. (23). Comparison of Eqs. (6) and (26) reveals that, as expected, the elastic flexibility matrix, a_E , appears in place of the inverse of the stiffness matrix, K^{-1} .

Force-derivative method (FDM)

The development of higher-order forms of the FDM is similar to the development for the MAM. First, Eq. (16) may be solved for $x_E(t)$ to yield

$$x_E(t) = \bar{K}_E^{-1} \Phi_E^T f(t) - \bar{K}_E^{-1} \bar{C}_E \dot{x}_E(t) - \bar{K}_E^{-1} \bar{M}_E \ddot{x}_E(t) \quad (27)$$

Assuming that the forcing function, $f(t)$ is sufficiently differentiable, Eq. (27) is then differentiated once with respect to time to obtain the following expression for $\dot{x}_E(t)$

$$\dot{x}_E(t) = \bar{K}_E^{-1} \Phi_E^T \dot{f}(t) - \bar{K}_E^{-1} \bar{C}_E \dot{x}_E(t) - \bar{K}_E^{-1} \bar{M}_E \ddot{x}_E(t) \quad (28)$$

If Eq. (27) is substituted into Eq. (20), the following expression is obtained

$$\begin{aligned} u(t) = & \Phi_R x_R(t) + a_E f(t) - \Phi_E \bar{K}_E^{-1} \bar{C}_E \bar{K}_E^{-1} \Phi_E^T \dot{f}(t) \\ & + (\Phi_E \bar{K}_E^{-1} \bar{C}_E \bar{K}_E^{-1} \bar{C}_E - \Phi_E \bar{K}_E^{-1} \bar{M}_E) \dot{x}_E(t) + (\Phi_E \bar{K}_E^{-1} \bar{C}_E \bar{K}_E^{-1} \bar{M}_E) \ddot{x}_E(t) \end{aligned} \quad (29)$$

Using the definitions given in Eqs. (17), Eq. (29) may be rewritten as

$$\begin{aligned} u(t) = & \Phi_R x_R(t) + a_E f(t) - a_E C a_E \dot{f}(t) \\ & + (\Phi_E \Omega_E^{-2} \Lambda_E \Omega_E^{-2} \Lambda_E - \Phi_E \Omega_E^{-2}) \dot{x}_E(t) + (\Phi_E \Omega_E^{-2} \Lambda_E \Omega_E^{-2}) \ddot{x}_E(t) \end{aligned} \quad (30)$$

To derive an expression for the FDM, a reduced set of modes and natural frequencies, damping coefficients and generalized coordinates are used in the last two terms in Eq. (30) to yield

$$\begin{aligned} u(t) = & \Phi_R x_R(t) + a_E f(t) - a_E C a_E \dot{f}(t) \\ & + (\hat{\Phi}_E \hat{\Omega}_E^{-2} \hat{\Lambda}_E \hat{\Omega}_E^{-2} \hat{\Lambda}_E - \hat{\Phi}_E \hat{\Omega}_E^{-2}) \dot{\hat{x}}_E(t) + (\hat{\Phi}_E \hat{\Omega}_E^{-2} \hat{\Lambda}_E \hat{\Omega}_E^{-2}) \ddot{\hat{x}}_E(t) \end{aligned} \quad (31)$$

Expressions for $\dot{\hat{x}}_E(t)$ and $\ddot{\hat{x}}_E(t)$ may be obtained from Eq. (24) by using Leibnitz's rule. The modified expression for the second-order form of the FDM may then be derived by substituting these expressions into Eq. (31). This expression is given in Eq. (32).

$$\begin{aligned} u(t) \approx & \Phi_R x_R(t) + \hat{\Phi}_E \hat{x}_E(t) + (a_E - \hat{\Phi}_E \hat{\Omega}_E^{-2} \hat{\Phi}_E^T) f(t) \\ & - (a_E C a_E - \hat{\Phi}_E \hat{\Omega}_E^{-2} \hat{\Lambda}_E \hat{\Omega}_E^{-2} \hat{\Phi}_E^T) \dot{f}(t) \end{aligned} \quad (\text{order 2}) \quad (32)$$

Comparing Eqs. (7) and (32) reveals that the elastic flexibility matrix, a_E , appears in place of the inverse of the stiffness matrix, K^{-1} .

Lanczos method

The modifications to the theory of the Lanczos method are analogous to those made for the MDM, the MAM, and the FDM. The rigid-body displacements used for this method are identical to those calculated for the MDM. Furthermore, by inspecting Eqs. (9) it is apparent that the theory for the Lanczos method contains terms that have a form similar to the static-displacement term, $K^{-1}f(t)$, that is present in the MAM and the FDM. Therefore,

the theory for the Lanczos method is modified by substituting the elastic flexibility matrix, a_E , for K^{-1} in Eqs. (9).

The displacements, $u(t)$, for the Lanczos method can be written as the sum of the rigid-body displacements and the elastic displacements, as shown in Eq. (33).

$$u(t) \approx u_R(t) + \hat{u}_E(t) \approx \Phi_R x_R(t) + \hat{Q}_E \hat{x}_E(t) \quad (33)$$

In Eq. (33), \hat{Q}_E and $\hat{x}_E(t)$ have definitions similar to those given for \hat{Q} and $\hat{x}(t)$ in Eqs. (9). The Lanczos coordinates, $\hat{x}_E(t)$, are calculated by integrating

$$\bar{M}_E \ddot{x}_E + \bar{C}_E \dot{x}_E + \bar{K}_E x_E = \Phi_E^T f(t) \quad (34)$$

where

$$\bar{M}_E = \hat{Q}^T M a_E M \hat{Q} = T_m \quad (35a)$$

$$\bar{C}_E = \hat{Q}^T M a_E C \hat{Q} \quad (35b)$$

$$\bar{K}_E = \hat{Q}^T M \hat{Q} = I \quad (35c)$$

and

$$\bar{f}_E(t) = \hat{Q}^T M a_E f(t) \quad (35d)$$

As stated previously, Eqs. (35) are obtained by substituting a_E for K^{-1} in Eqs. (9). The displacements, $u(t)$, are then calculated by substituting the Lanczos coordinates, $\hat{x}_E(t)$, into Eq. (33). This method may be considered to be a hybrid modal-Lanczos method since it uses both rigid-body modes and Lanczos vectors in the analysis.

Determination of the Basis Vectors and Computational Procedures

The four reduced-basis methods discussed in the present paper, as well as the direct integration of the full system of equations of motion by the Newmark-Beta time integration method, have been implemented on high-performance computers and incorporated into the COmputational MEchanics Testbed (COMET) general purpose finite element code.⁹ The computational times presented are for a CONVEX C220 high-performance computer.

The Lanczos vectors are computed by an eigensolver which is based on the Lanczos algorithm described in references 15-18. Furthermore, it was shown in references 17-18 that computing the natural frequencies and eigenvectors of a structural system from a set of Lanczos vectors is much more computationally efficient than using subspace iteration. The Lanczos-vector-based eigensolver described in references 17-18 was implemented to take advantage of the capabilities of high-performance computers, particularly those with vector capabilities; therefore, it was also used to compute the natural frequencies and eigenvectors for the example problems presented in the present paper.

The integration of Eqs. (14), (16) and (27) to calculate the rigid-body coordinates, the elastic modal coordinates and the Lanczos coordinates, respectively, is carried out using the Newmark-Beta implicit time-integration method. The values of α , β , and Δt are identical to those for the full-system solution.

The computational procedures followed for the calculations involving the elastic flexibility matrix, a_E , are described subsequently. The direct calculation of the a_E matrix using Eq. (23) requires that the flexibility matrix, a , (i.e., $a = K^{-1}$) be found relative to a set of statically determinate constraints. This calculation would require a computationally intensive direct inversion of the stiffness matrix. However, a significant amount of CPU time can be saved by recognizing that the a_E matrix usually appears in the equations in terms that are matrix-vector products, as in the elastic static displacement term, $a_E f(t)$, that appears in Eq. (26). This elastic static displacement term may be rewritten by substituting the definition of a_E (Eq. (23)) into it to yield

$$a_E f(t) = R^T a R f(t) \quad (36)$$

Therefore, the direct inversion of the stiffness matrix may be avoided by first computing the product $R f(t)$, and then performing a static solution relative to the aforementioned statically determinate constraints to generate the product $K^{-1} R f(t)$, or $a R f(t)$. The elastic static displacement term may then be calculated using Eq. (36) by premultiplying the product $a R f(t)$ by R^T .

A procedure similar to that just described may be used to compute the \bar{C}_E term defined in Eq. (35b) for use with the Lanczos method. If the definition of a_E given in Eq. (23) is substituted into Eq. (35b), the following equation is obtained:

$$\bar{C}_E = \hat{Q}^T M R^T a R C \hat{Q} \quad (37)$$

The most important difference in the procedure to calculate this term is that the number of static solutions that must be performed relative to the statically determinate constraints is equal to m , the number of basis vectors being used in the approximate solution. The calculation of the elastic static displacement term described previously requires only one static solution. The right-hand-side vectors for the m static solutions required to calculate \bar{C}_E are the columns of the $(n \times m)$ matrix defined by the product $R C \hat{Q}$. These solutions yield the product $K^{-1} R C \hat{Q}$ or $a R C \hat{Q}$. The calculation of \bar{C}_E is then completed by premultiplying the product $a R C \hat{Q}$ by the product $\hat{Q}^T M R^T$. Additional discussion of the other computational procedures followed in the implementation of the reduced-basis methods is given in reference 8.

Spatial Error Norm

The accuracy of the transient response calculated using the reduced-basis methods was evaluated quantitatively using a relative, spatial error norm defined in references 12-14. Since the error norm selected is a spatial error norm, it is calculated at only one point in time. The error norm used to evaluate the approximate displacement solutions (referred to as the displacement error norm) is defined in Eq. (38).

$$e_u = \sqrt{\frac{\delta^T \delta}{u_f^T u_f}} \quad (38)$$

where

e_u is the displacement error norm

$\delta = u_f - u_a$

u_f is the displacement vector obtained from the full-system solution

and

u_a is the displacement vector obtained from an approximate solution using a reduced set of basis vectors.

Similarly, a moment error norm, e_M , and a stress error norm, e_S , may be obtained using Eq. (38) and replacing the displacement vectors with vectors containing either nodal moment values or values of stress. The nodal moment values and the stress values for all of the methods (including the full-system solution) are computed by back substituting the displacement response solutions into a stress post-processor in the COMET code. A discussion of the effectiveness of the error norm in measuring the accuracy of the approximate solutions is given in reference 8. In reference 8, an error limit was established for the purposes of comparison. The value of this error limit was set equal to 0.01, and, in the present study, the approximate solutions obtained using the reduced-basis methods will be considered to be converged when the value of the error norm is equal to or less than this value.

Results and Discussion

Two example problems are presented to verify the four modified reduced-basis methods and to compare the convergence and computational time requirements of each of the methods. The first example problem is an unconstrained beam subject to a uniformly distributed load which varies as a sinusoidal function of time. The second example problem is an unconstrained high-speed civil transport aircraft subject to a normal wing tip load which also varies as a sinusoidal function of time. The beam problem is a simple example of the application of the modified theory, and the high-speed civil transport problem is an example of the application of these methods for the analysis of more complex, built-up structures. The transient responses of both structures

calculated using the reduced-basis methods are verified with and compared to the full-system solution obtained by integrating directly the full system of equations of motion.

Results are presented which compare the number of basis vectors required by each of the methods to reach a predetermined error limit corresponding to a given value of the spatial error norm. Furthermore, computational times required for each of the methods to reach the predetermined error limit are presented and compared.

Unconstrained beam subject to a uniformly distributed load

The free-free beam example problem is illustrated in figure 1. The finite element model of the beam consists of 51 nodes and 50 planar beam elements. Each of the 51 nodes has two degrees-of-freedom, and there is a total of 102 degrees-of-freedom. The material properties, span length and moment of inertia are all prescribed to have values of unity ($E = 1 \text{ lb/in}^2$, $\rho = 1 \text{ lb}_m/\text{in}^3$, $L = 1 \text{ in.}$ and $I = 1 \text{ in}^4$). The forcing function, $f(t)$, selected for this example varies as a sinusoidal function of time and is defined by $f(t) = 1000 \sin(20t)$, where t is time. The forcing frequency, $\omega_f = 20 \text{ rad/sec}$, was selected to be less than the first non-zero natural frequency of the beam, which is $\omega_3 = 22.37 \text{ rad/sec}$ (3.561 Hz).

Convergence of approximate responses

A plot of the displacement error norm, e_U , as a function of the number of basis vectors, m , is shown in figure 2 for the unconstrained beam example. The results shown in the figure are for the MDM, MAM, FDM (order 4 and 6) and the Lanczos method at time $t = 1.0 \text{ sec}$. The horizontal line at a value of $e_U = 10^{-2}$ on the ordinate represents the value of the previously described error limit, and error values on and below this line represent a calculated response that has negligible or acceptable error.

As shown in figure 2, the MAM, the FDM (order 4), and the FDM (order 6) each converge to the prescribed error limit using only one mode or basis vector. The Lanczos method requires two basis vectors for convergence, and the MDM requires three modes or basis vectors for convergence. It is apparent that for this example problem, all of the methods are effective in representing the transient displacements using a small number of basis vectors.

The moment error norm, e_M , as a function of the number of basis vectors, m , is shown in figure 3. The results are presented at time $t = 1.0 \text{ sec}$ for the same methods used in figure 2. The Lanczos method converges to the prescribed error limit using two basis vectors. The MAM, the FDM (order 4), and the FDM (order 6) each requires three modes or basis vectors for convergence. However, the MDM, requires 25 modes or basis vectors for convergence. The poor convergence of the moment solution illustrated by the MDM is not unusual since the moments depend on the second derivative of the displacements, and any errors that are present in the displacements will be magnified by the derivative process.

Computational time requirements

A comparison of the computational time (i.e., CPU time) required for each method to yield converged displacement solutions is presented in Table I. The CPU times given in Table I are normalized with respect to the CPU time required to obtain the full-system solution, and they are for the first occurrence of a value of e_U less than the predefined error limit of 0.01. The number of basis vectors is the number required for each method to reach the value of e_U that is given in the table. The times given for the modal methods include the time required for the computation of the specified number of natural frequencies and eigenvectors using the Lanczos-vector-based eigensolver, and the time shown for the Lanczos method includes the time for the eigensolver to compute the specified number of Lanczos vectors. The time to compute the rigid-body displacements and the a_E matrix is also included in the times given for the Lanczos method. As shown in Table I, all four of the reduced-basis methods require approximately the same amount of CPU time to obtain converged displacement solutions, with the Lanczos method requiring the least amount of time.

A similar comparison of the normalized CPU time required for each method to obtain converged moment solutions is presented in Table II. The CPU times presented are for the first occurrence of a value of e_M less than the predefined error limit $e_M = 0.01$. All four of the reduced-basis methods require a similar amount of CPU time, with the Lanczos method requiring the smallest amount of time to obtain converged moment solutions.

High-speed civil transport aircraft subject to a normal wing-tip load

The high-speed civil transport aircraft example problem represents a larger, more realistic and complex structure, and is illustrated in figure 4. Only half of the structure is modeled to take advantage of the physical symmetry. A plane of symmetry is defined on the centerline running down the length of the model. The model is otherwise unconstrained. The finite element model contains 398 nodes and 1323 rod, beam, membrane and shear elements. Each of the nodes has four unconstrained degrees-of-freedom, and, excluding the symmetry constraints, there is a total of 1316 degrees-of-freedom. The forcing function, $f(t)$, acts normal to the wing tip (i.e., in the z-direction), and the amplitude varies as a sinusoidal function of time defined by $f(t) = 1000 \sin(10t)$, where t is time. The forcing frequency, $\omega_f = 10$ rad/sec, was selected to be less than the first non-zero natural frequency of the aircraft, which is $\omega_4 = 14.14$ rad/sec (2.251 Hz). Damping is not considered in this example.

Convergence of approximate responses

A plot of the displacement error norm, e_U , as a function of the number of basis vectors, m , is shown in figure 5 for the high-speed civil transport example. The results shown in the figure are for the MDM, MAM, FDM (orders 3 and 5) and the Lanczos method at time $t = 1.0$ sec. As shown in figure 5, the MAM and the FDM (orders 3 and 5) converge using only one mode or basis vector. The MDM requires two modes or basis vectors for convergence, and the Lanczos method requires five modes or basis vectors for convergence.

The moment error norm, e_M , as a function of the number of basis vectors, m , is shown in figure 6 for the high-speed civil transport example problem. The values of stress used in Eq. (37) are the membrane stresses in the wing and fuselage cover panels. These cover panels were modeled in the finite element model using membrane elements. The results are presented at time $t = 1.0$ sec for the same methods used in figure 5. The MAM and the FDM (order 3 and 5) each require two modes or basis vectors to converge to the error limit, the Lanczos method requires nine basis vectors, and the MDM requires ten modes or basis vectors to converge. The poorer convergence of the stresses when compared to the convergence of the displacements is not unusual since the values of stress depend upon the second derivative of the displacements.

Computational time requirements

A comparison of the normalized CPU time required for each method to yield converged displacement solutions is presented in Table III. As shown in Table III, the MDM requires the smallest amount of CPU time to obtain converged displacement solutions. The MAM and the Lanczos method each require approximately the same amount of time, and the FDM (order 3 and 5) requires the largest amount of time. A large portion of the added computational time required for the MAM, the FDM (orders 3 and 5) and the Lanczos method is spent on the calculations involving the a_E matrix. Therefore, since the MAM and the Lanczos method each require one calculation involving the a_E matrix, it is reasonable that these two methods require approximately the same amount of CPU time. The CPU time requirements for the FDM (orders 3 and 5) are increased over those for the other methods because the FDM requires several more calculations involving the a_E matrix as the order of the method used is increased.

A comparison of the normalized CPU time required for each method to obtain converged stress solutions are presented in Table IV. The CPU times presented are for the first occurrence of a value of e_s less than the predefined error limit $e_s = 0.01$. As with the displacements, the MDM requires the smallest amount of CPU time to obtain converged displacement solutions. The MAM and the Lanczos method each require approximately the same amount of time, and the FDM (order 3 and 5) requires the largest amount of time. However, the CPU times required by all four reduced-basis methods to obtain converged displacement and stress solutions are significantly less than the CPU time required to obtain the corresponding full-system solutions.

Concluding Remarks

The present study develops, verifies, and compares two advanced reduced-basis methods and two lower-order modal methods for linear transient structural analysis of unconstrained structures. The advanced reduced-basis methods studied are a higher-order modal method referred to as the force-derivative method (FDM), and the Lanczos method, a reduced-basis method that uses Lanczos vectors as basis vectors. The lower-order modal methods are the mode-displacement method (MDM) and the mode-acceleration method (MAM).

The modifications made to the theory for these methods to allow for the analysis of unconstrained structures are presented and discussed.

Solutions from the four methods are verified with a full-system solution obtained by directly integrating the full system of equations of motion using the Newmark-Beta implicit time integration method. The accuracy of the approximate responses have been measured using a relative, spatial error norm. Computational time for the four methods as well as the full-system solution are compared. The results from the methods have been compared for two example problems: an unconstrained beam subject to a uniformly distributed load which varies as a sinusoidal function of time and an unconstrained high-speed civil transport aircraft subject to a normal wing tip load which varies as a sinusoidal function of time. The scope of these two example problems is not intended to be an exhaustive study since several problem parameters were not considered. The parameters not included in the present study are: the time variation of the forcing function, the inclusion of different types of damping (i.e., proportional and non-proportional), and the spatial distribution of the forcing function.

All four of the reduced-basis methods are shown to require very few basis vectors and approximately the same amount of CPU time to obtain converged displacement solutions for the unconstrained beam problem. The number of basis vectors required by the MDM to obtain converged moment solutions is significantly larger than that required to obtain converged displacements. However, the CPU times required by all of the methods to obtain converged moment solutions are very nearly equal.

The MAM and the FDM with the inclusion of third- and fifth-order terms have been found to require the fewest number of basis vectors to obtain converged displacement and stress solutions for the unconstrained high-speed civil transport example. However, the CPU time required to calculate the terms involving an elastic flexibility matrix, a_E , increases the solution time required for these modal methods. This elastic flexibility matrix has been used to eliminate the need to compute the inverse of the stiffness matrix. Increases in the CPU time required for the Lanczos method also occur because of the calculations involving a_E . Therefore, since the MDM requires a relatively small number of basis vectors to obtain converged displacement and stress solutions for this example, it requires smaller amounts of CPU time than the MAM, the FDM and the Lanczos method.

In general, it is concluded that the MAM and the higher-order modal method (FDM) offer an advantage in terms of the number of basis vectors required to obtain converged solutions. However, due to the computational requirements associated with the calculations involving the elastic flexibility matrix, the CPU time requirements for the FDM will be greater than those for the MAM. The Lanczos method does not offer an advantage over the MAM or the FDM in terms of the number of basis vectors required to obtain converged solutions. Furthermore, the CPU time requirements for the Lanczos method are, in general, similar to those for the MAM. For large problems with rigid-body modes, the MDM may require the smallest amount of CPU time if it is able to obtain converged solutions with a relatively small number of modes.

References

1. Meirovitch, L.: *Analytical Methods in Vibrations*. The MacMillan Company, c.1967.
2. Biot, M. A. and Bisplinghoff, R. L.: *Dynamic Loads on Airplane Structures During Landing*. NACA Wartime Report W-92, October, 1944.
3. Williams, D.: Displacements of a Linear Elastic System Under a Given Transient Load – Part I. *The Aeronautical Quarterly*, vol. 1, August 1949, pp. 123-136.
4. Cornwell, R. R.; Craig, R. R., Jr.; and Johnson, C. P.: On The Application of the Mode-Acceleration Method to Structural Engineering Problems. *Earthquake Engineering and Structural Dynamics*, vol. 11, 1983, pp. 679-688.
5. Wilson, E. L.; Yuan, M. W.; and Dickens, John M.: Dynamic Analysis by Direct Superposition of Ritz Vectors. *Earthquake Engineering and Structural Dynamics*, vol. 10, 1982, pp. 813-821.
6. Nour-Omid, Bahram and Clough, Ray W.: Dynamic Analysis of Structures Using Lanczos Coordinates. *Earthquake Engineering and Structural Dynamics*, vol. 12, No. 4, July-August, 1984, pp. 565-577.
7. Kline, K. A.: Dynamic Analysis Using a Reduced Basis of Exact Modes and Ritz Vectors. *AIAA Journal.*, vol. 24, no.12, December, 1986, pp. 2022-2029.
8. McGowan, David M. and Bostic, Susan W.: Comparison of Advanced Reduced-Basis Methods for Transient Structural Analysis. *AIAA Paper 91-1059*, April 1991.
9. Stewart, Caroline B., Compiler: *The Computational Structural Mechanics Testbed User's Manual*. NASA TM 100644, October, 1989.
10. Craig, Roy R., Jr.: *Structural Dynamics-An Introduction to Computer Methods*, John Wiley & Sons, Inc., New York, New York, c.1981.
11. Cook, Robert D.: *Concepts and Applications of Finite Element Analysis*, John Wiley & Sons, New York, New York, c.1981.
12. Camarda, C. J. and Haftka: R. T.,: *Development of Higher-Order Modal Methods for Transient Thermal and Structural Analysis*. NASA TM 101548, February, 1989.
13. Camarda, C. J.; Haftka, R. T.; and Riley, M. F.: An Evaluation of Higher-Order Modal Methods for Calculating Transient Structural Response. *Computers & Structures*, vol. 27, no. 1, 1987, pp. 89-101.

14. Camarda, C. J.: *Development of Advanced Modal Methods for Calculating Transient Thermal and Structural Response*. NASA TM 104102, December, 1991.
15. Lanczos, C.: An Iteration Method for the Solution of the Eigenvalue Problem of Linear Differential and Integral Operators. *Journal of Research, National Bureau of Standards*, vol. 45, 1950, pp. 255-282.
16. Chen, Harn C. and Taylor, Robert L.: Solution of Eigenproblems for Damped Structural Systems by the Lanczos Algorithm. *Computers & Structures*, vol. 30, no. 1/2, 1988, pp. 151-161.
17. Bostic, Susan W.: A Vectorized Lanczos Eigensolver for High-Performance Computers. AIAA Paper 90-1148, April 1990.
18. Bostic, Susan W. and Fulton, R.E.: Implementation of the Lanczos Method on a Parallel Computer. *Computers & Structures*, vol. 25, no. 3, 1987, pp. 395-403.

Table I. Comparison of CPU times at first occurrence of $e_U < 0.01$ for the free-free beam example.

| Method | No. of Basis Vectors | $e_U \times 10^{-3}$ | Normalized CPU time ^a |
|----------------------|----------------------|----------------------|----------------------------------|
| MDM (order 0) | 3 | 4.375 | 0.2673 |
| MAM (order 1) | 1 | 1.540 | 0.2528 |
| FDM (order 4) | 1 | 1.194 | 0.2624 |
| FDM (order 6) | 1 | 1.185 | 0.2695 |
| Lanczos | 2 | 0.3494 | 0.2430 |
| Full-System Solution | - | - | 1.000 |

a CPU times normalized with respect to the full-system solution time

Table II. Comparison of CPU times at first occurrence of $e_M < 0.01$ for the free-free beam example.

| Method | No. of Basis Vectors | $e_M \times 10^{-3}$ | Normalized CPU time ^a |
|----------------------|----------------------|----------------------|----------------------------------|
| MDM (order 0) | 25 | 9.292 | 0.4960 |
| MAM (order 1) | 3 | 5.717 | 0.3298 |
| FDM (order 4) | 3 | 5.383 | 0.3404 |
| FDM (order 6) | 3 | 5.354 | 0.3432 |
| Lanczos | 2 | 7.239 | 0.2890 |
| Full-System Solution | - | - | 1.000 |

a CPU times normalized with respect to the full-system solution time

Table III. Comparison of CPU times at first occurrence of $e_U < 0.01$ for the high-speed civil transport aircraft example.

| Method | No. of Basis Vectors | $e_U \times 10^{-3}$ | Normalized CPU time ^a |
|----------------------|----------------------|----------------------|----------------------------------|
| MDM (order 0) | 2 | 4.030 | 0.02765 |
| MAM (order 1) | 1 | 5.486 | 0.06908 |
| FDM (order 3) | 1 | 4.161 | 0.1073 |
| FDM (order 5) | 1 | 3.962 | 0.1462 |
| Lanczos | 5 | 5.073 | 0.06753 |
| Full-System Solution | - | - | 1.000 |

^a CPU times normalized with respect to the full-system solution time.

Table IV. Comparison of CPU times at first occurrence of $e_S < 0.01$ for the high-speed civil transport aircraft example.

| Method | No. of Basis Vectors | $e_U \times 10^{-3}$ | Normalized CPU time ^a |
|----------------------|----------------------|----------------------|----------------------------------|
| MDM (order 0) | 10 | 9.454 | 0.06317 |
| MAM (order 1) | 2 | 8.847 | 0.08229 |
| FDM (order 4) | 2 | 8.127 | 0.1202 |
| FDM (order 6) | 2 | 8.097 | 0.1558 |
| Lanczos | 9 | 5.959 | 0.08688 |
| Full-System Solution | - | - | 1.000 |

^a CPU times normalized with respect to the full-system solution time.

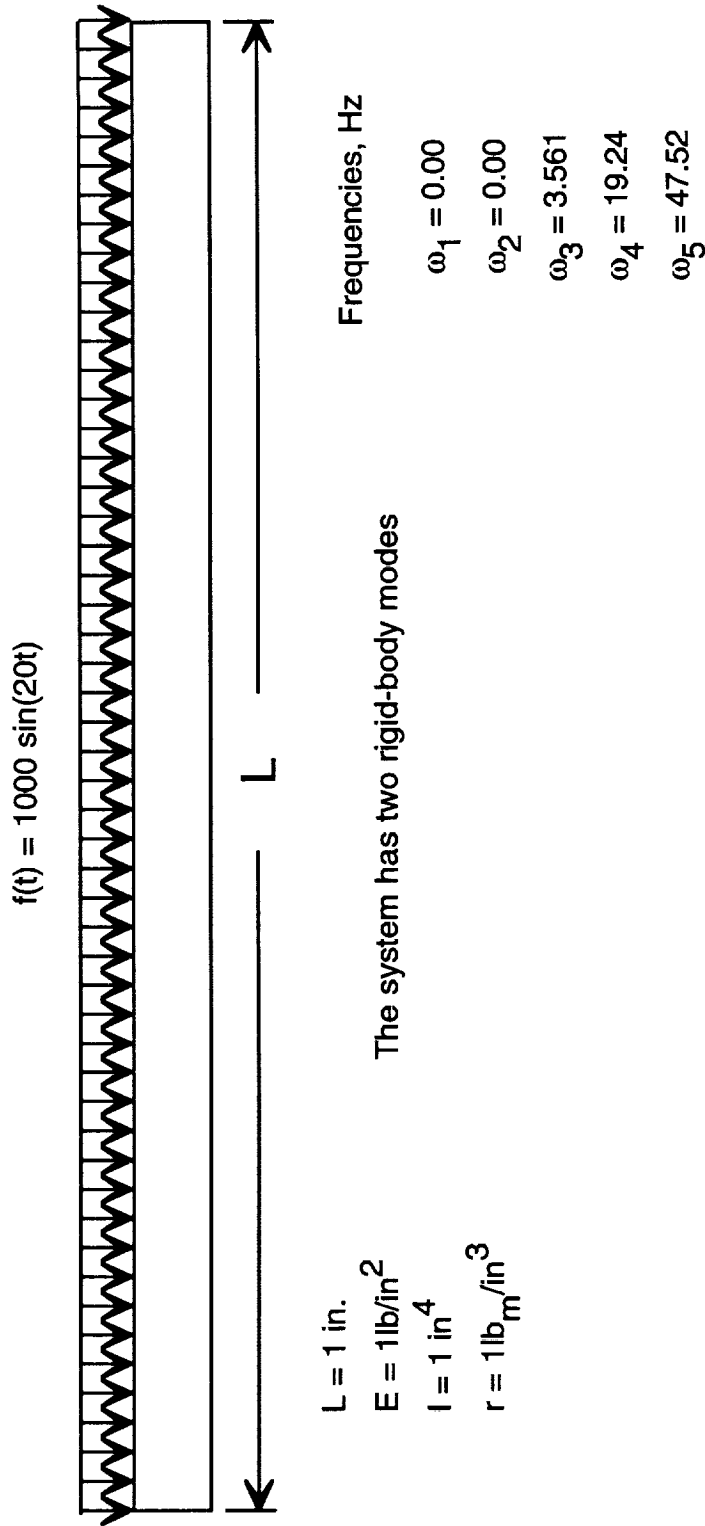


Figure 1. - Unconstrained beam subject to a uniformly distributed load that varies as a sinusoidal function of time.

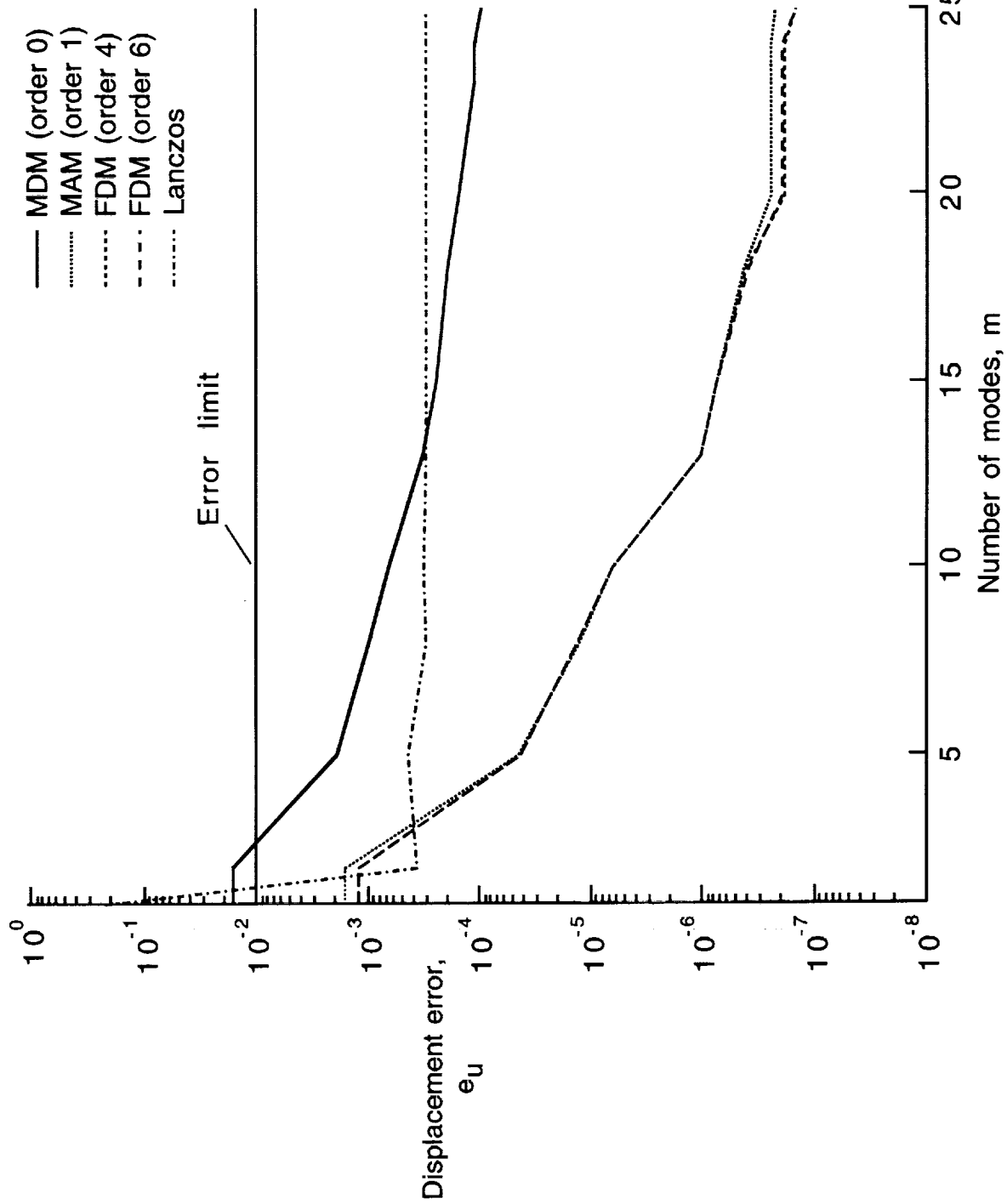


Figure 2. - Convergence of displacements for the unconstrained beam illustrated in Fig. 1 ($t = 1.0$ sec).

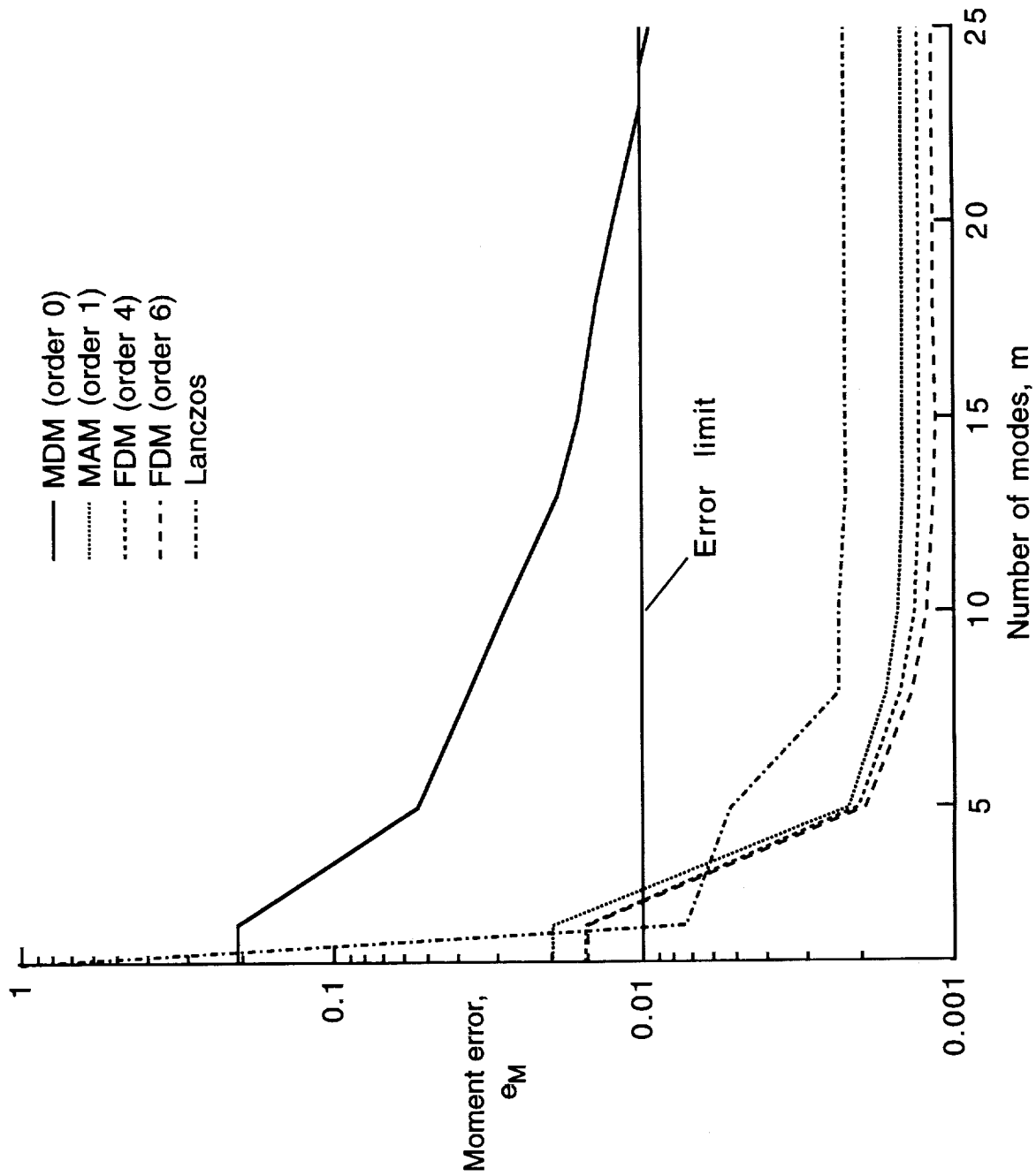


Figure 3. - Convergence of moments for the unconstrained beam illustrated in Fig. 1 ($t = 1.0$ sec).

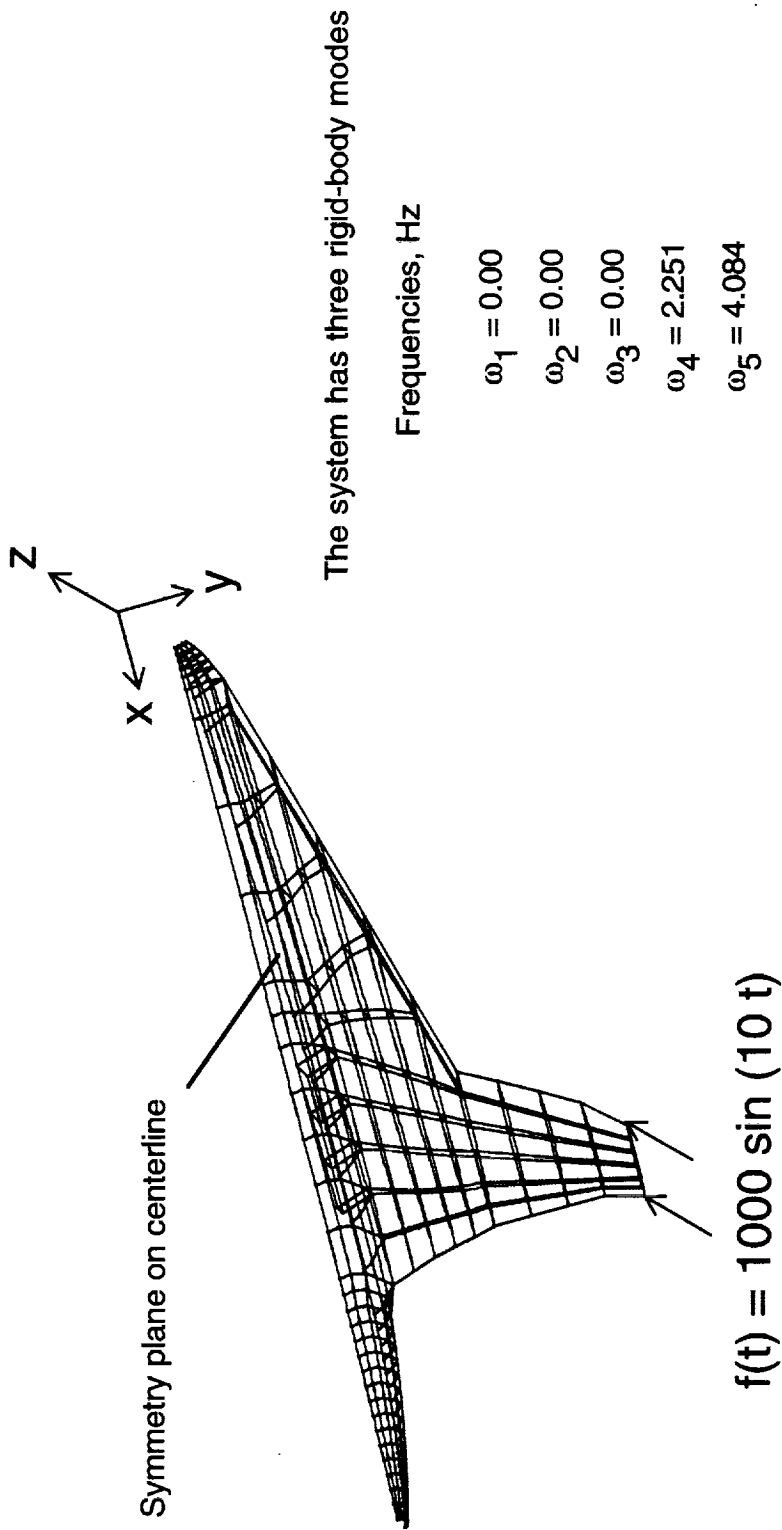


Figure 4. - Unconstrained high-speed civil transport wing and fuselage subject to a normal wing-tip load that varies as a sinusoidal function of time.

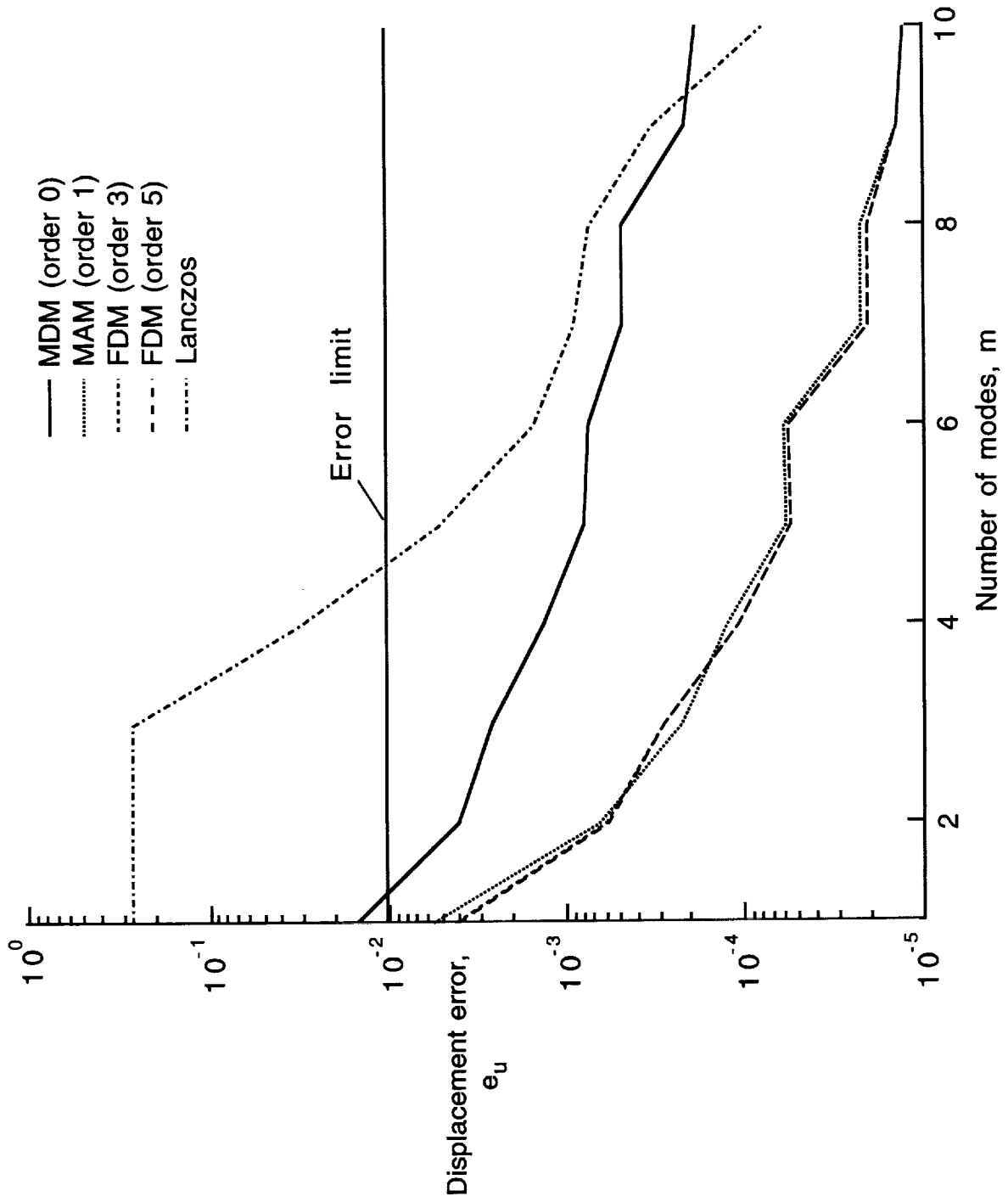


Figure 5. - Convergence of displacements for the unconstrained high-speed civil transport illustrated in Fig. 4 ($t = 1.0$ sec).

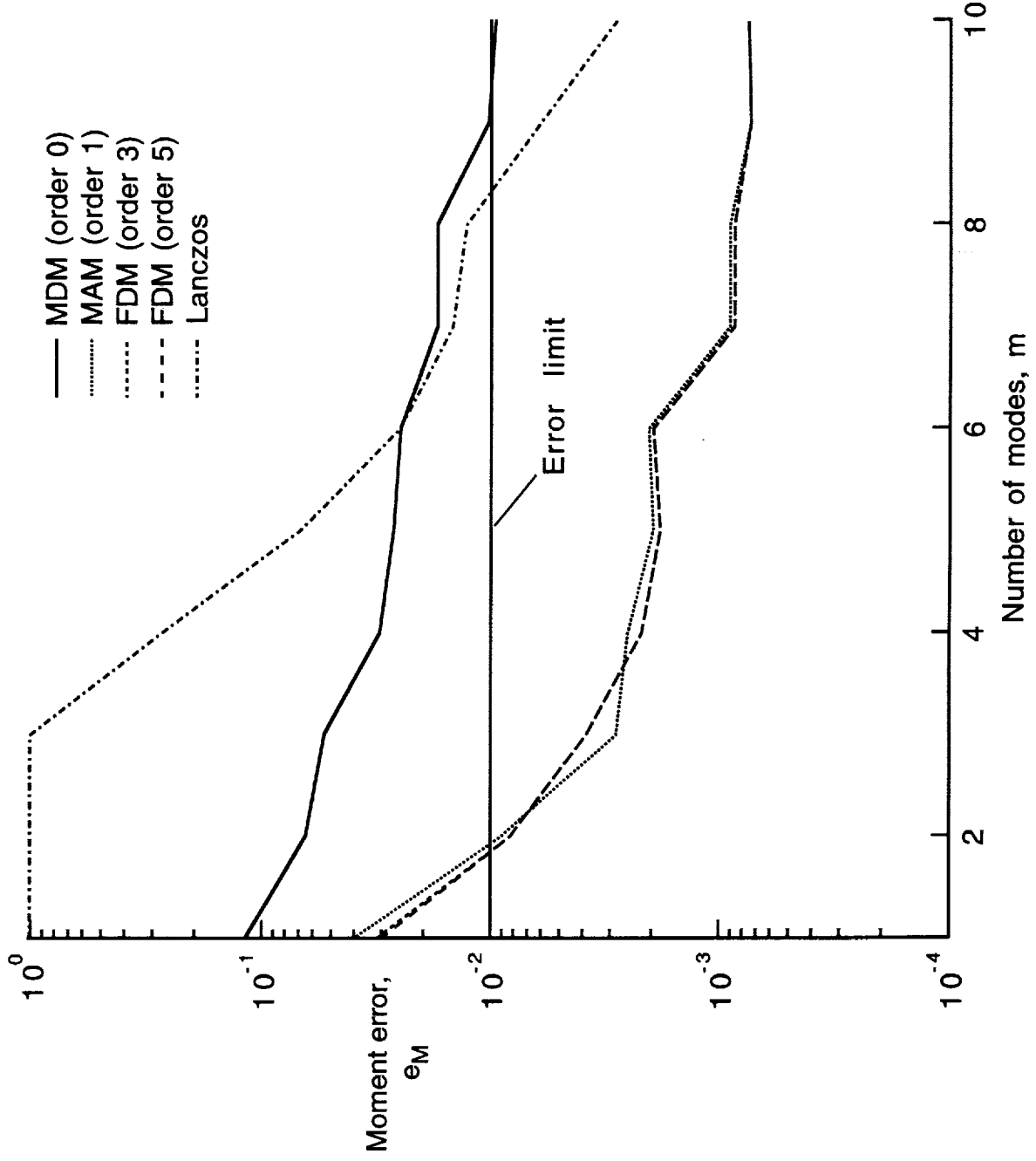


Figure 6. - Convergence of moments for the unconstrained high-speed civil transport illustrated in Fig. 4 (t = 1.0 sec).

REPORT DOCUMENTATION PAGE

Form Approved
OMB No. 0704-0188

Public reporting burden for this collection of information is estimated to average 1 hour per response, including the time for reviewing instructions, searching existing data sources, gathering and maintaining the data needed, and completing and reviewing the collection of information. Send comments regarding this burden estimate or any other aspect of this collection of information, including suggestions for reducing this burden, to Washington Headquarters Services, Directorate for Information Operations and Reports, 1215 Jefferson Davis Highway, Suite 1204, Arlington, VA 22202-4302, and to the Office of Management and Budget, Paperwork Reduction Project (0704-0188), Washington, DC 20503.

| | | | | |
|---|--|---|--|--|
| 1. AGENCY USE ONLY (Leave blank) | | 2. REPORT DATE November 1993 | 3. REPORT TYPE AND DATES COVERED Technical Memorandum | |
| 4. TITLE AND SUBTITLE Development and Comparison of Advanced Reduced-Basis Methods for the Transient Structural Analysis of Unconstrained Structures | | | 5. FUNDING NUMBERS WU 537-06-21-09 | |
| 6. AUTHOR(S) David M. McGowan Susan W. Bostic Charles J. Camarda | | | 8. PERFORMING ORGANIZATION REPORT NUMBER | |
| 7. PERFORMING ORGANIZATION NAME(S) AND ADDRESS(ES) NASA Langley Research Center Hampton, VA 23681-0001 | | | | |
| 9. SPONSORING / MONITORING AGENCY NAME(S) AND ADDRESS(ES) National Aeronautics and Space Administration Washington, DC 20546-0001 | | | 10. SPONSORING / MONITORING AGENCY REPORT NUMBER NASA TM-109015 | |
| 11. SUPPLEMENTARY NOTES | | | | |
| 12a. DISTRIBUTION / AVAILABILITY STATEMENT Unclassified - Unlimited Subject Category - 39 | | | 12b. DISTRIBUTION CODE | |
| 13. ABSTRACT (Maximum 200 words) The development of two advanced reduced-basis methods, the force-derivative method and the Lanczos method, and two widely used modal methods, the mode-displacement method and the mode-acceleration method for transient structural analysis of unconstrained structures is presented. Two example structural problems are studied; an undamped, unconstrained beam subject to a uniformly distributed load which varies as a sinusoidal function of time and an undamped high-speed civil transport aircraft subject to a normal wing tip load which varies as a sinusoidal function of time. These example problems are used to verify the methods and to compare the relative effectiveness of each of the four reduced-basis methods for performing transient structural analyses on unconstrained structures. The methods are verified with a solution obtained by integrating directly the full system of equations of motion, and they are compared using the number of basis vectors required to obtain a desired level of accuracy and the associated computational times as comparison criteria. | | | | |
| 14. SUBJECT TERMS Lanczos vectors, transient structural analysis, unconstrained structures, rigid-body modes, modal superposition/acceleration | | | 15. NUMBER OF PAGES 29 | |
| | | | 16. PRICE CODE A03 | |
| 17. SECURITY CLASSIFICATION OF REPORT Unclassified | 18. SECURITY CLASSIFICATION OF THIS PAGE Unclassified | 19. SECURITY CLASSIFICATION OF ABSTRACT Unclassified | 20. LIMITATION OF ABSTRACT | |